

Article

New SRR/CSRR antenna dual Band-notch for WLAN and X Band Satellite communication

El Amjed Hajlaoui¹ , Ziyad Almohaimeed¹ 

¹Department of Electrical Engineering, College of Engineering, Qassim University, 51452, Saudi Arabia, hajlamjed@yahoo.fr, z.mohaimeed@qu.edu.sa

Abstract— This paper will propose an innovative compact, low-cost, low-profile inverted U-shaped patch antenna with a single and dual band-notched ultra-wideband (UWB) with split ring resonators (SRRs). To achieve our main goal based on the reduction of electromagnetic interference in narrowband communications (WLAN, WiMAX, and satellite), four-element rectangular split-ring resonators (SRRs) array are placed nearby the feedline to create notch band at approximately 5.15-5.35 and 5.725-5.85 GHz. The SRRs antenna's measured data indicate a directivity of 8.52 dBi, a gain of 7.18 dBi, a reflection coefficient of -27 dB, and an efficiency of 84.3%. The realized prototype, including the SRRs and CSRRs structures, were carried out using a PCB prototyping machine. Reflection coefficient measurement is obtained using a vector network analyzer (VNA) PNA-X from Agilent Technologies. The measured values of the proposed antenna, with 50 x 38 x 1.6 mm³ in total and constructed on a FR4 substrate with permittivity of $\epsilon_r = 4.3$, loss $\tan\delta = 0.0024$ and substrate thickness of $h = 1.6$ mm, correlate well with the simulated values. The proposed antenna, compared with other published work, is a good candidate to operate in WLAN, X-band.

Index Terms—split ring resonator (SRR); Ultra-wideband (UWB) antenna; WLAN; X-band.

I. INTRODUCTION

Interest in ultra-wideband (UWB) systems has recently increased because of their low power consumption, affordable cost, high data throughput capabilities, little interference, and precise position. These systems have been allowed to operate in the 3.1 to 10.6 GHz frequency spectrum for UWB systems as written in [1]. On the other hand, narrowband systems operate within this frequency range. Consequently, UWB devices must avoid interfering with these narrowband systems; using a UWB antenna equipped with a band-reject capability solves this problem. Additionally, these systems need a short-size UWB antenna with a flat group delay [2]-[8].

This article has merged a split ring resonator (SRR) that is sometimes called negative refractive index materials [9], [10]. SRRs are based on a couple of concentric annular rectangular rings with opposite ends, as shown in Fig. 1. Consequently, a magnetic field (H) vertically applied to the square ring surface will produce currents that will push out a magnetic field that may decrease or enhance the incident field,

given the structure's resonant properties. On the other side, we can acquire the complementary split-ring resonator (CSRRs) by engraving SRRs in the ground.

The proposed antenna will combine dual-band and SRR structures, as shown in Fig. 1, with a full size of $50 \times 38 \times 1.6 \text{ mm}^3$. The dual resonant structures allow the proposed antenna to operate in two bands that can be easily adjusted by modifying associated SRR structure parameters.

Our main objective in this paper is to apply new techniques based on this SRR to design single and dual band-notched UWB antennas in different bands according to our implementation. The first technique will permit obtaining the band notch for the 5.15-5.35 GHz and hyperactive line frequency bands, 5.72-5.85 GHz, by inserting four SRRs near the feed line. The second will be founded on the etching of the ground plane with complementary SRRS (CSRR) to realize X-band satellite communication and WLAN rejection.

II. SINGLE BAND REJECTION BASED ON SRR STRUCTURES

In this section, an equalization methodology exploiting Split Ring Resonators (SRRs) is proposed in this work. SRR, presented here in Fig. 1, can be parasitically coupled to the antenna. Their configuration can be controlled so that the scattered eld can constructively add to the one radiated by the antenna.

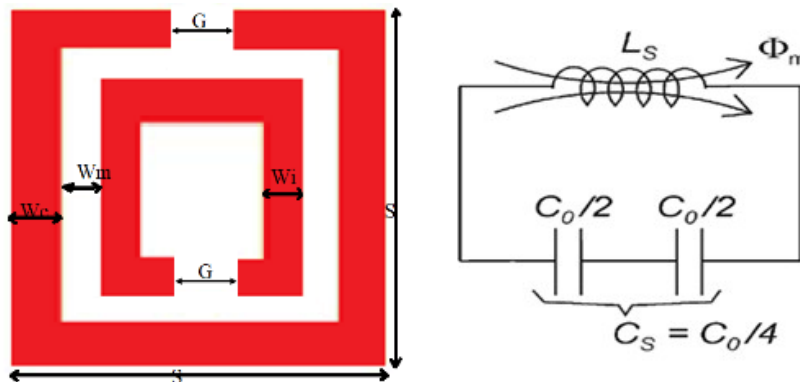


Fig.1. Split-ring-resonator and its equivalent circuit

Split ring resonator is used to build left hand material. SRR unit is an artificial magnetic resonator which resonates at a frequency with a λ_0 that is much larger than the SRR length. The resonance occurs when a time varying magnetic field is applied perpendicular to the plane that contains the SRR units. This results in inducing circulating surface currents on its rings, and the distribution of these currents shows that charges of opposite sign accumulated across the gaps and form a large distributed capacitance, which in turn results in producing very high positive and negative values of effective permeability at the desired frequency where SRR strongly resonates. The permeability and permittivity of circular SRR can be extracted from simulated scattering parameter data S11 and S21 while assuming adopting adequate geometric parameters given Table 1.

TABLE I. DIMENSION PROPOSED OF THE SRR (MM)

Parameter	Dimension (mm)
We	0.2
Wi	0.2
Wm	0.2
S	1.46
G	0.2

To verify the antenna model performance characteristics, initially simulation of unit cell was carried on CST tool and presented in Fig. 2 and Fig. 3. Permeability and permittivity with respect to the unit cell analysis are showing the negative values.

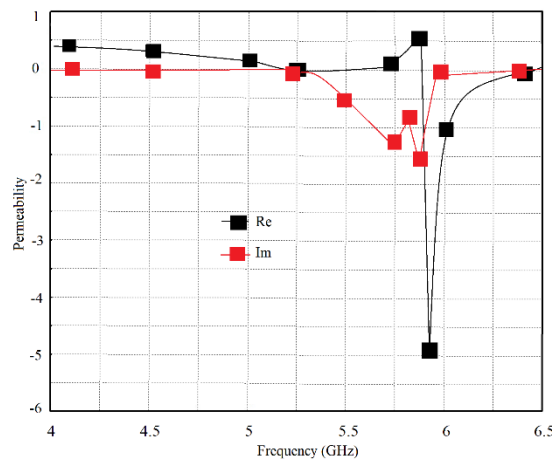


Fig. 2. CST simulation of the SRR permeability unit cell along the desired band.

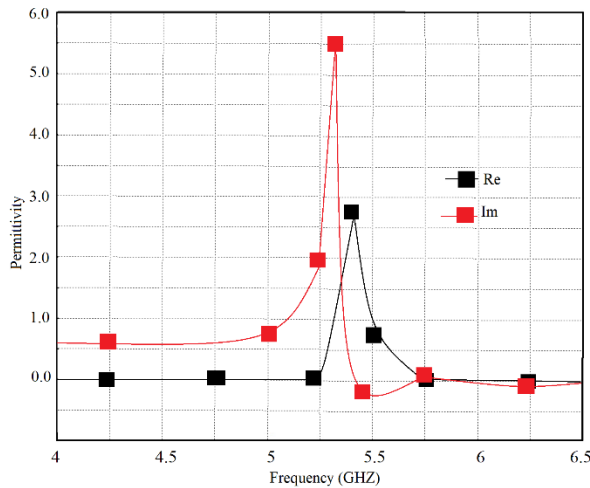


Fig. 3 . CST simulation of the permittivity SRR unit cell along the desired band.

The use of parasitically coupled radiators is widely exploited in conventional microstrip antennas and it has been applied to a variety of antenna geometries [11]-[13]. In general, coupled radiating elements are used for gain improvement, to enlarge the operating band, or for reconfigurability purposes. The resonant frequency of the SRRs depends on their size and on the gap capacitance. Here, the SRRs affect

the antenna performance in two ways. They act as a parasitic radiator and then contribute to the overall antenna gain in relation to their resonance frequency. In the other side, their coupling to the antenna, depending on the distance g , affects the input impedance and reflection coefficient.

The inverted U-shaped patch antenna depicted in Fig. 4 (a) was prototyped on an FR4 substrate with permittivity of $\epsilon_r = 4.3$, loss $\tan\delta = 0.0024$ and substrate thickness of $h = 1.6$ mm. Four element array of a rectangular SRR will be placed near the feedline as shown in Fig. 4 (b)

Table II presents the geometric parameters of the whole structure results of optimization to control the desired resonance frequency and the features of UWB.

TABLE II. DIMENSION OF THE PROPOSED ANTENNA

Parameters	Dimensions (in mm)	Parameters	Dimensions (in mm)
W_p	30	a	1.5
L_p	24	c	1
L_g	13.5	d	0.18
W_f	2.85	g	0.4
L_f	14	r	4
L_s	50	s	0.275
W_s	38	w	0.4
a	1.5	h	1.6

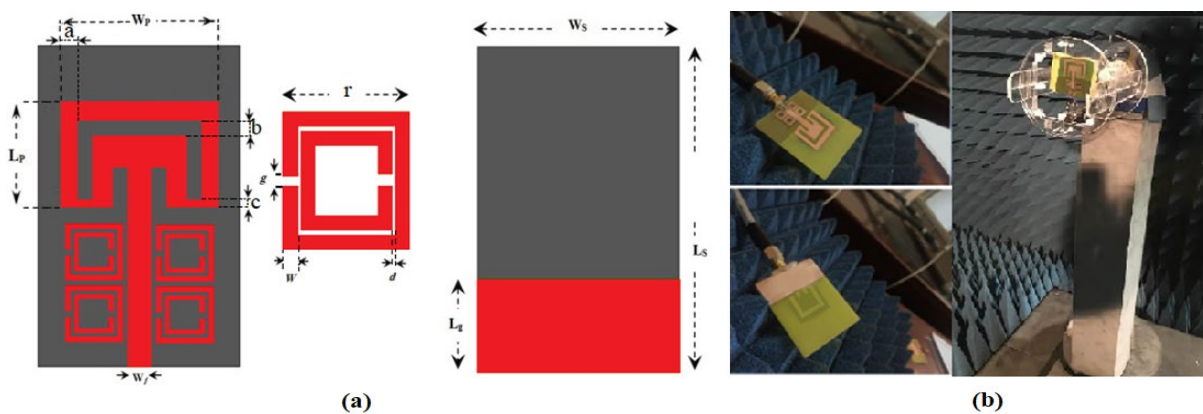


Fig. 4. (a) Proposed SRR inverted U-shaped UWB band notch antenna (b) its realized prototype

When included, the four rectangular SRRs, integrated with the inverted U-shaped antenna, will permit a single band-notched antenna structure inside the WLAN band (5.15-5.85 GHz).

The reflection coefficient of the proposed antenna depicted in Fig. 5, shows that the WLAN band contains the single band-notch, and Fig. 6 indicates gain estimated at 5dB.

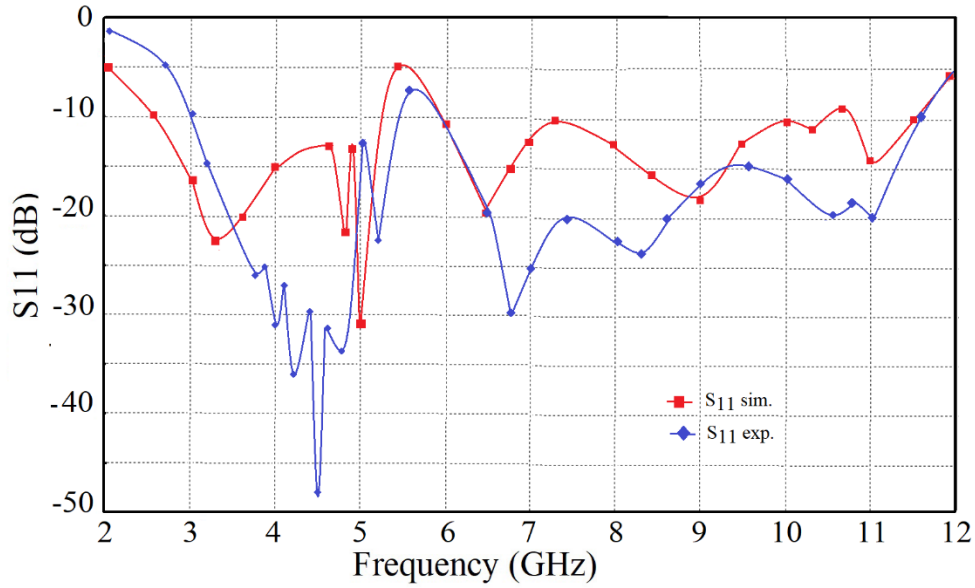


Fig. 5. reflection coefficient of the conventional SRR inverted U-shaped UWB band notch antenna.

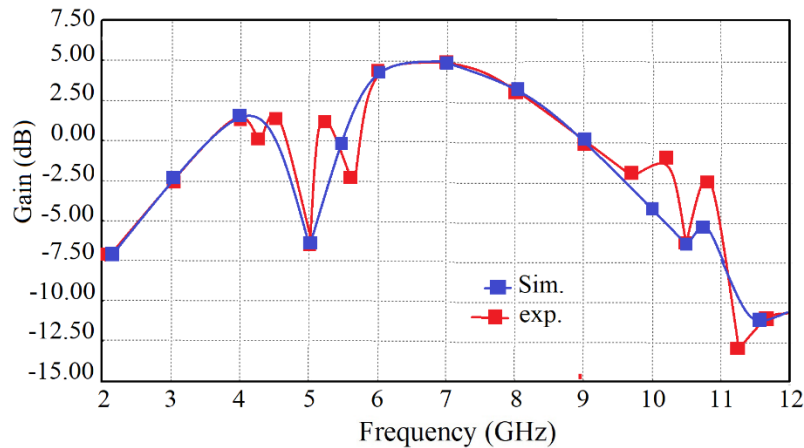


Fig. 6. Peak realized gain of the proposed SRR inverted U-shaped UWB band notch antenna. red simulated and blue measured results

III. DOUBLE BAND REJECTION BASED ON THE IMPLEMENTATION OF CSRR STRUCTURES AS DEFECTED GROUND SURFACES ON THE INVERTED U-SHAPED ANTENNA

Altering our traditional inverted U-shaped antenna by etching these similar structures into the ground is another method of rejecting the WLAN spectrum (4.85–6.1 GHz). This antenna will be referred to as the complement SRR structures (CSRR) in Fig. 7. To achieve WLAN frequency band rejection, it is important to optimize these novel CSRR structures. Here, we must first put one cell to see what effect it has, but we will not alter the proportions of our suggested inverted U-shaped antenna throughout the entirety of our work.

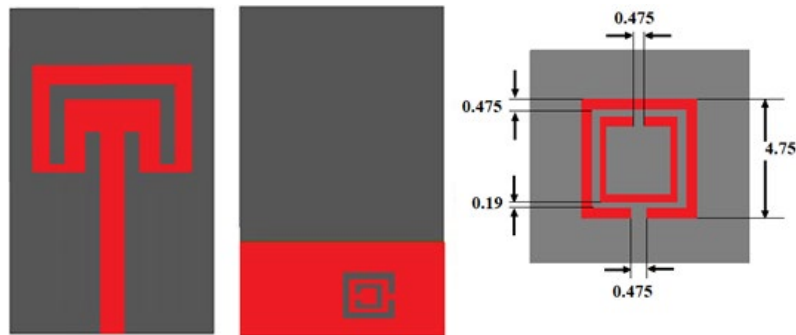


Fig. 7. Conventional inverted U-shaped antenna with CSRR structures (in mm)

The CSRR structure of a standard loaded inverted U-shaped antenna is simulated, revealing a rejection bandwidth of 4.5 to 4.9 GHz and a resonance frequency of 4.7 GHz. To accomplish the WLAN stopband, sufficient redistribution of CSRR on the traditional antenna should be considered.

The standard loaded inverted U-shaped antenna CSRR's scattering parameter (S_{11}) reveals a resonance frequency that spans the WLAN band rejection of 4.9 GHz–5.9 GHz and occurs before the stopband. Furthermore, as illustrated in Fig. 8, the development of the non-desirable band rejection (8 to 8.5 GHz reach to 10 dB) has a significant impact on the reflection coefficient performance of the inverted U-shaped antenna with only one CSRR structure inserted.

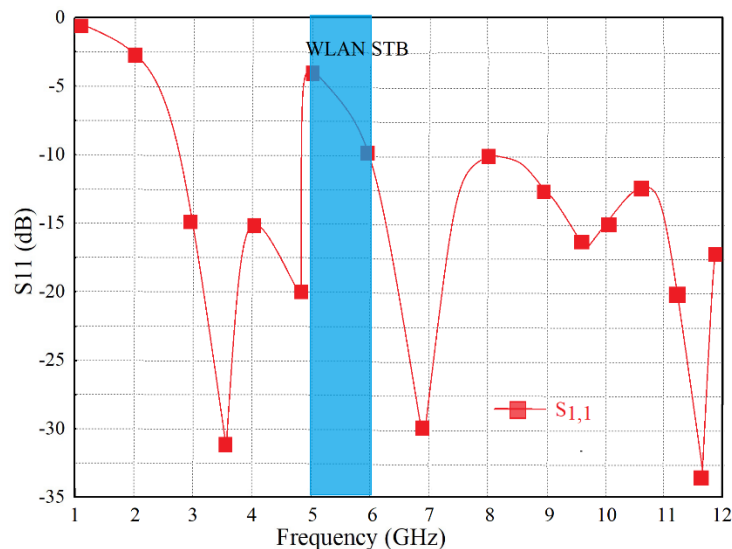


Fig. 8. Scattering parameter S_{11} of the inverted U-shaped antenna, including one CSRR cell.

An optimization of a single CSRR dimension is carried out to cover the entire X-Band. The quantity of CSRR cells must then be increased. The geometric dimensions of the single-cell will be determined by a new parametric research to $r=3.2$ mm, $w=0.32$ mm, $d=0.128$ mm, and $g=0.32$ mm in order to preserve the reflection coefficient and all X-band rejection of our typical inverted U-shaped antenna.

Two supplementary CSRR cells, as shown in Fig. 9, are inserted at a distance of 1.6 mm, from the feed center, to prevent any perturbations in the given output parameters and create another stopband.

Previous analysis [14] shows that two stopband regions will appear via the scattering parameters when 3 CSRR cells are loaded near the microstrip feed. The first one is due to the insertion of the first CSRR cell, and the second region will consequently appear when we have inserted the two other CSRR cells. These cells have a 7.9 GHz resonance frequency and a wavelength of 7.5 to 8.2 GHz.

As shown in Fig. 9, the geometry of these 3 CSRR cell will permit to control the WLAN frequency band rejection and to cover the entire X-band.



Fig. 9. The inverted U-shaped antenna with the three CSRR cells and their prototype

The scattering parameter S_{11} , presented in Fig. 10, for the conventional antenna loaded 3 CSRR cells has one stopband, WLAN band rejection, that goes from 4.85 to 5.9 GHz, while the other stopband goes from 7.1 to 8.125 GHz.

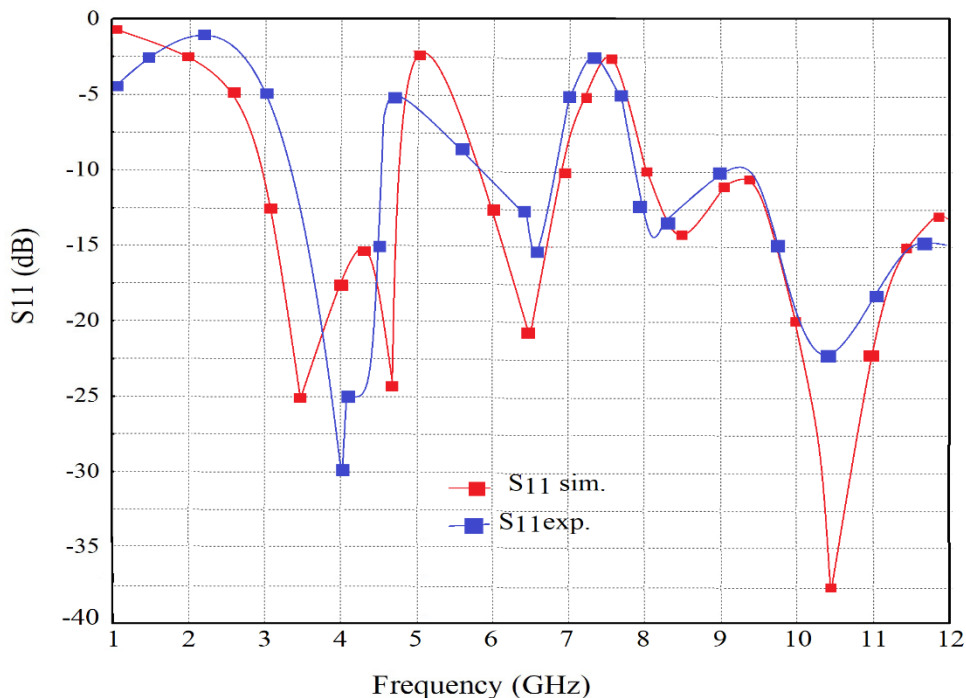


Fig. 10. Comparison between simulation and measurement results of the inverted U-shaped UWB antenna while using CSRRs structures.

These are representatives of the downlink (7.25-7.75 GHz) and the majority of the uplink (7.9–8.4 GHz) X-band. Furthermore, there was an overall enhancement of the reflection coefficient performance of our inverted U-shaped conventional antenna due to the loss of the undesirable band rejection (8 to 8.5 GHz reach to 10 dB) that was first observed during the loading of a single CSRR.

Three loaded CSRR cells must be rearranged throughout the conventional antenna in order to maintain WLAN band rejection and X-band rejection while avoiding any Return Los reflection coefficient antenna performance disturbances.

Here, as shown in Fig. 11, the gain is equal to 6.6dB at 6.4 GHz. For the two rejected bands as a result of the CSRR impact, a respectable gain drop was seen at two central frequencies (0.46dB at 4.9 GHz and -4.9dB at 7.55 GHz).

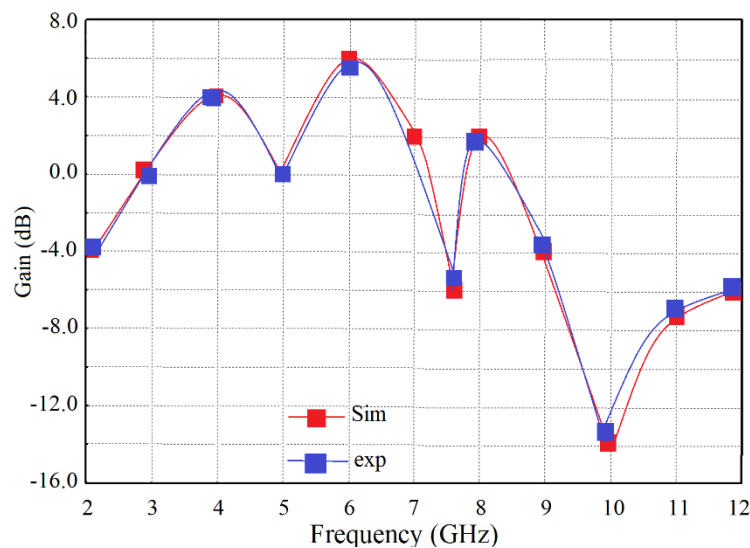


Fig. 11. Summit gain response of conventional antenna with 3 CSRR cells loaded. red simulated and blue measured results

With the exception of the frequency band-notch, the two suggested UWB antenna-based CSRRs and UWB antenna-based SRRs—present extremely high radiation efficiency levels of 95.5% and 94% in all frequency bands. As a result, there will be substantially fewer electromagnetic wave interference in the X-band and WLAN for satellite communications. The insertion of the SRR and CSRR structures leads to the radiation efficiency behavior in the band-notch frequencies.

Through the insertion of these SRR and CSRRs beside/below the line of the feed, the band-notch UWB antennas discussed in our research show greater gain and stability while maintaining compactness as compared to other documented references, such as referenced [15], [16]. When we incorporate a combination of SRR and CSRR structures into a single inverted U-shaped UWB antenna, both the modeling and measurement results of the two approaches are evaluated in Fig. 12.

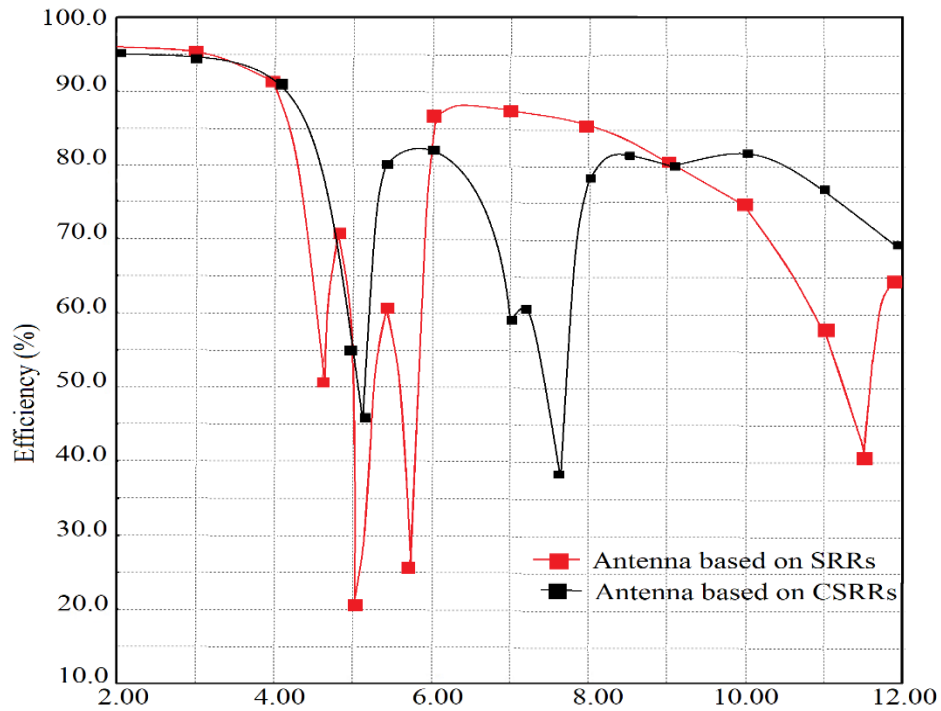


Fig. 12. Radiation efficiency of the both proposed configurations of the proposed antenna

The efficiency of the two proposed antenna configurations is shown in Fig. 12. The first was based on SRRs, while the second was solely based on CSRRs. Exceptionally high radiation efficiencies were recorded in all frequency bands except the frequency band-notch, with maximum values of 95.5% and 94% for the first and second antenna, respectively. It therefore reduces electromagnetic wave interference in WLAN and X-band for satellite communications, when combining the two configurations together in our design. The insertion of the SRR and CSRR structures causes the loss of antenna matching inside these bands, which in turn affects the behavior of radiation efficiency in the band-notch frequencies.

The divergence between simulations and measurements is due to an anechoic chamber misalignment not being considered while using the software. Such presented in Fig. 13, when we illustrate the measured radiation pattern in the produced prototype's. Here, Fig. 13 (a), Fig. 13 (c) and Fig. 13 (e) represent the E-plane radiation pattern for the resonance frequencies 3.5 GHz, 6.5 GHz and 10 GHz respectively. However, Fig. 13 (b), Fig. 13 (d) and Fig. 13 (f) represent the H-plane radiation pattern of our CSSR Ultra Wide Band antenna for the same resonance frequencies.

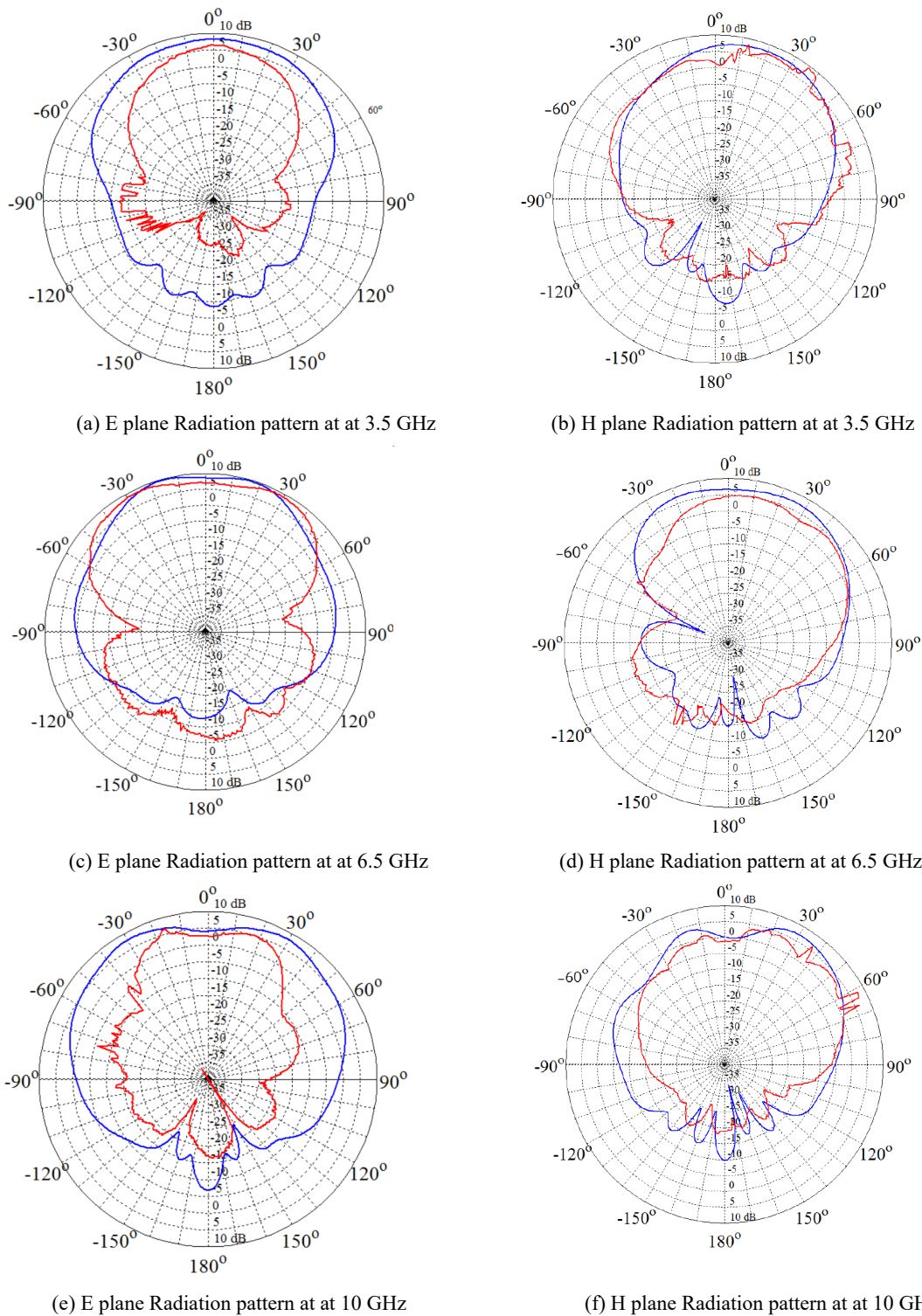


Fig. 13. E and H plane Radiation pattern of the Inverted CSRR- band-notched UWB antenna prototype for different frequency bands (Blue simulated, and red measured results)

Anechoic chamber measurements of the recommended antenna's radiation characteristic for co- and cross-polarizations are shown for a range of frequencies in Fig.9. The simulated and measured radiation properties in the two planes, shown in Fig. 13. XZ (E-field) and Y Z (H-field), accord well with the suggested antenna. The suggested antenna radiation pattern, which is necessary for these kind of Ultra

Wide Band band antenna, is similar to an omnidirectional antenna in the E-field (XZ plane) and H-field (YZ plane). Excellent level of consistency between the simulated and measured outcomes despite minor discrepancies. Potential reasons for this include mismatches between the SMA connectors, manufacturing errors, or losses in the copper, substrate, or SMA connection. Furthermore, the radiation is delivered in two main planes (H-plane and E-plane). Normalized simulated and measured radiation patterns at the operating frequencies of 3.5, 6.5, and 10.0 GHz show that the antenna retains its Omnidirectional behavior in the H-plane at lower frequencies despite slight cross-polarization fluctuation. However, at higher frequencies, the radiation pattern deteriorates owing to changes in the area of radiation.

IV. COMPARATIVE ANALYSIS

Table III illustrates a performance comparison between the proposed antenna and state-of-the-art antennas dedicated to the same applications. The antenna outperformed the existing antennas with its compact size, wider operating bandwidth, higher gain and stop-band functionality.

TABLE III. PERFORMANCE COMPARISON WITH STATE OF THE ART ANTENNAS

Ref. No.	Dimension (mm)	FBW (%)	Operating frequency (GHz)	Peak Gain (dbi)	Function Stop-band
[17]	30*31*1.5	136	3.1- 10.6	4.29	Yes
[18]	50*24*1.6	144	3.1- 10.66	5.78	Yes
[19]	80*67*3.4	124	3.7-10.3	4.53	No
[20]	30*22*0.8	75.40	2.9-6.41	4.6	Yes
[21]	44*30.5*1.5	-	3.1-10.6	6	Yes
Our approach	30*24*1.6	154.56	3.1- 10.6	7.18	Yes

V. CONCLUSION

A new SRR/CSRR inverted U-shaped UWB antenna design, measuring 50*38*1.6 mm³, has been shown. The proposed antennas cover services including close-range radar satellite communication and show suitable impedance matching characteristics over the operational spectrum of 3.1 to 10.6 GHz, including two high rejection notch bands, WLAN, and X-band satellite systems in UWB. The structural modification in the radiation patch increases impedance bandwidth by about 154.56% without affecting its size. The proposed antenna is an excellent candidate in comparison with other published works.

ACKNOWLEDGMENT

The author gratefully acknowledge Qassim University, represented by the Deanship of Scientific Research, on the financial support for this research.

REFERENCES

- [1] Federal communications commission: first report and order on ultra-wideband technology, FCC02-48, Washington, DC, pp. 34852-34860, 2002.
- [2] Y. -Y. Liu and Z. -H. Tu, "Compact Differential Band-Notched Stepped-Slot UWB-MIMO Antenna with Common-Mode Suppression," *IEEE Antennas and Wireless Propagation Letters*, vol. 16, pp. 593-596, 2017. doi: 10.1109/LAWP.2016.2592179.

- [3] B. Wu, X. -Y. Sun, H. -R. Zu, H. -H. Zhang and T. Su, "Transparent ultra wideband Halved Coplanar Vivaldi Antenna with Metal Mesh Film," *IEEE Antennas and Wireless Propagation Letters*, vol. 21, no. 12, pp. 2532-2536, 2022. doi: 10.1109/LAWP.2022.3200455.
- [4] X. Shan and Z. Shen, "Miniaturized UHF/UWB Tag Antenna for Indoor Positioning Systems," *IEEE Antennas and Wireless Propagation Letters*, vol. 18, no. 12, pp. 2453-2457, 2019. doi: 10.1109/LAWP.2019.2938808.
- [5] M. Rahman, A. Haider and M. Naghshvarianjahromi, "A Systematic Methodology for the Time-Domain Ringing Reduction in UWB Band-Notched Antennas," *IEEE Antennas and Wireless Propagation Letters*, vol. 19, no. 3, pp. 482-486, 2020. doi: 10.1109/LAWP.2020.2972025.
- [6] R. B. V. B. Simorangkir, A. Kiourti and K. P. Esselle, "UWB Wearable Antenna with a Full Ground Plane Based on PDMS-Embedded Conductive Fabric," *IEEE Antennas and Wireless Propagation Letters*, vol. 17, no. 3, pp. 493-496, 2018. doi: 10.1109/LAWP.2018.2797251.
- [7] C. Zhang, Y. Xie, Y. Wang, L. Dai and L. Niu, "Novel Miniaturized All-Metal UWB Magneto-Electric Monopole (MEM) Antenna for Multistandard Applications," *IEEE Transactions on Antennas and Propagation*, vol. 69, no. 7, pp. 4195-4200, 2021. doi: 10.1109/TAP.2020.3044710.
- [8] G. Srivastava, A. Mohan and A. Chakrabarty, "Compact Reconfigurable UWB Slot Antenna for Cognitive Radio Applications," *IEEE Antennas and Wireless Propagation Letters*, vol. 16, pp. 1139-1142, 2017. doi: 10.1109/LAWP.2016.2624736.
- [9] G. Zamora, S. Zuffanelli, P. Aguilà, F. Paredes, F. Martín and J. Bonache, "Broadband UHF-RFID Passive Tag Based on Split-Ring Resonator (SRR) and T-Match Network," *IEEE Antennas and Wireless Propagation Letters*, vol. 17, no. 3, pp. 517-520, 2018. doi: 10.1109/LAWP.2018.2800166.
- [10] J. Naqui, M. Duran-Sindreu and F. Martin, "Modeling Split-Ring Resonator (SRR) and Complementary Split-Ring Resonator (CSRR) Loaded Transmission Lines Exhibiting Cross-Polarization Effects," *IEEE Antennas and Wireless Propagation Letters*, vol 12, pp. 178-181, 2013.
- [11] M. Khalily, R. Tafazolli, P. Xiao and A. A. Kishk., "Broadband mm-Wave Microstrip Array Antenna With Improved Radiation Characteristics for Different 5G Applications," *IEEE Transactions on Antennas and Propagation*, vol. 66, no. 9, pp. 4641-4647, 2018. doi: 10.1109/TAP.2018.2845451.
- [12] Melvin C. Jose, S.Radha, B.S.Sreeja, and Pratap Kumar., "Design of 28 GHz high gain 5G MIMO antenna array system," *IEEE Region 10 Conf. (TENCON)*, pp. 1913–1916, 2018. doi.org/10.1109/TENCON.2019.8929690
- [13] J. Kumar, B. Basu, F. A. Tlukdar, A. Nandi., "Multimode-Inspired Low Cross-Polarization Multiband Antenna Fabricated Using Graphene-Based Conductive Ink," *IEEE Antennas Propag. Lett.*, vol. 17, pp. 1861-1865, 2018.
- [14] M. A. H. Ansari, A. K. Jha, Z. Akhter and M. J. Akhtar, "Multi-Band RF Planar Sensor Using Complementary split ring resonator for Testing of Dielectric Materials," *IEEE Sensors Journal*, vol. 18, no. 16, pp. 6596-6606, 2018. doi: 10.1109/JSEN.2018.2822877.
- [15] H. Huang, Y. Liu, S. Zhang and S. Gong, "Uniplanar Differentially Driven Ultra Wideband Polarization Diversity Antenna with Band-Notched Characteristics," *IEEE Antennas and Wireless Propagation Letters*, vol. 14, pp. 563-566, 2015. doi: 10.1109/LAWP.2014.2374332.
- [16] I. B. Vendik, A. Rusakov, K. Kanjanasit, J. Hong and D. Filonov, "Ultra wideband (UWB) Planar Antenna with Single-, Dual-, and Triple-Band Notched Characteristic Based on Electric Ring Resonator," *IEEE Antennas and Wireless Propagation Letters*, vol. 16, pp. 1597-1600, 2017. doi: 10.1109/LAWP.2017.2652978.
- [17] Rahman, M.; NaghshvarianJahromi, M.; Mirjavadi, S.S.; Hamouda, A.M."Compact UWB Band-Notched Antenna with Integrated Bluetooth for Personal Wireless Communication and UWB Applications," *Electronics*, vol. 8, issue 2, 158, 2019. doi.org/10.3390/electronics8020158
- [18] Mandal, T.; Das, S. "Design of a microstrip fed printed monopole antenna for bluetooth and UWB applications with WLAN notch band characteristics," *Int. J. RF Microw. Comput. Eng.*, vol 25, pp. 66–74, 2015.
- [19] Simorangkir, R.B.V.B.; Kiourti, A.; Esselle, K. "UWB Wearable Antenna with a Full Ground Plane Based on PDMS-Embedded Conductive Fabric," *IEEE Antennas Wirel. Propag. Lett.*, vol. 17, pp. 493–496, 2018.
- [20] Mohammad Alibakhshi-Kenari, Mohammad Naser-Moghadasi, R.A. Sadeghzadeh. "Bandwidth and radiation specifications enhancement of monopole antennas loaded with split ring resonators," *IET Microwaves, Antennas & Propagation*. Vol 9, Issue 14, pp. 1487-1652, 2015. doi.org/10.1049/iet-map.2015.0172
- [21] Rahman, M., NaghshvarianJahromi M., Mirjavadi, S.S., Hamouda, A.M. "Resonator Based Switching Technique between Ultra Wide Band (UWB) and Single/Dual Continuously Tunable-Notch Behaviors in UWB Radar for Wireless Vital Signs Monitoring," *Sensors*. Vol. 18, issue 10, 3330, 2018. doi.org/10.3390/s18103330